IEEE Access
Multidisciplinary ⋮ Rapid Review ⋮ Open Access Journal

Received January 5, 2022, accepted February 4, 2022, date of publication February 15, 2022, date of current version March 1, 2022.

Digital Object Identifier 10.1109/ACCESS.2022.3151685

Extraction of Forestry Parameters Based on Multi-Platform LiDAR

JIANCHANG CHEN[1,2,3,4], YIMING CHEN[1], AND ZHENGJUN LIU[1]

[1]Chinese Academy of Surveying and Mapping, Beijing 100830, China
[2]Faculty of Geomatics, Lanzhou Jiaotong University, Lanzhou, Gansu 730070, China
[3]National and Local Joint Engineering Research Center for the Application of Geographical Situation Monitoring Technology, Lanzhou, Gansu 730070, China
[4]Gansu Provincial Engineering Laboratory of Geographical Situation Monitoring, Lanzhou, Gansu 730070, China

Corresponding author: Zhengjun Liu (zjliu@casm.ac.cn)

This work was supported in part by the National Key Research and Development Program of China under Grant 2018YFB0504504, in part by the National Natural Science Foundation of China under Grant 41730107, in part by the Funded Project of Fundamental Scientific Research Business Expenses of Chinese Academy of Surveying and Mapping under Grant AR2104, and in part by the Lanzhou Jiaotong University (LZJTU) under Grant 201806.

ABSTRACT Quick and accurate acquisition of tree height (TH) and diameter at breast height (DBH) plays a very important role in forestry surveys. These parameters can be collected rapidly and accurately with LiDAR. In this paper, an accurate tree parameters extraction method with combining the use of Unmanned Aerial Vehicle Laser Scanning (UAVLS) to extract TH and Terrestrial Laser Scanning (TLS) to extract DBH was proposed. To verify the applicability of this method, this paper collected LiDAR data in the Laohugou forest area (a natural forest) and Saihanba forest area (an artificial forest), Hebei Province, China. For the extraction of TH, both forest areas had overestimated. The coefficient of determination R^2 of TH in Laohugou forest area was 0.9458 and the root mean square error (RMSE) was 0.7 m, while in Saihanba forest area R^2 was 0.95 and the RMSE was 0.65 m. A method based on point density analysis was proposed to automatically extract DBH. First, the data by TLS was normalized and made four-centimeter slices at 1.3 m. Then, branches, weeds and outliers were eliminated using an improved K-means algorithm. Finally, point density analysis was performed on all sections, and threshold values were set to automatically complete the extraction of DBH. The automatic DBH extraction by this paper proposed method was consistent with the actual measurements, and the mean intersection over union (MIOU) reached 89%. The R^2 of DBH in the Laohugou forest area was 0.9941 and the RMSE was 0.65 cm; the R^2 of DBH in the Saihanba forest area was 0.99 and the RMSE was 0.43 cm. These results confirm that the accurate extraction of DBH in two forest areas with different growth conditions and different tree species.

INDEX TERMS LiDAR, forestry, point cloud, parameter extraction.

I. INTRODUCTION

The increase in population, the burning of fossil fuels, and deforestation of forest resources have caused an excess of carbon dioxide in the atmosphere, intensifying the problem of global warming [1]–[3]. Quick and effective access to various types of ecological information can provide theoretical basis and scientific guidance for policymakers to formulate policies for sustainable development, alleviating climate warming, and maintaining the balance of the ecosystem. Forests are an important part of the natural ecosystem. Forests mainly absorb carbon dioxide from the atmosphere, regulate the carbon-water balance, and play an important role in mitigating global warming and balance ecosystems [4]. Tree height (TH) and diameter at breast height (DBH) are one of the most important attributes in forest resource surveys. These two parameters and other tree parameters (tree species, crown width, etc.) are often used to predict forest storage capacity and carbon sequestration capacity [5], [6]. Therefore, fast and accurate acquisition of forestry parameter is of great significance to forestry resource assessment and management.

Traditionally, forestry resource surveys based on field visits to measure trees, which were characterized by low efficiency and heavy workloads [6], [7]. Forestry resource surveys of virgin forests also present harsh environments and a high risk of injury. In recent 20 years, remote sensing technology has become one of the important means to obtain information on the structure, change and distribution of forest

The associate editor coordinating the review of this manuscript and approving it for publication was Hongjun Su.

resources by virtue of its rapid, accurate, and non-destructive acquisition of tree data at multiple spatial scales [8]. LiDAR technology is an emerging active remote sensing technology that acquires information by emitting laser beams and receiving echo signals. LiDAR technology can be used to rapidly obtain accurate three-dimensional information of objects and has been widely used in forestry resource surveys. According to the platform involved, LiDAR technology mainly can be divided into Spaceborne Laser Scanning (SLS), Airborne Laser Scanning (ALS), and Terrestrial Laser Scanning (TLS). SLS is mainly used for global or regional forestry resource surveys. Due to the low point density, the accuracy of SLS data collection is low [9], [10]. ALS is divided into Manned Aerial Vehicle Laser Scanning (MAVLS) and Unmanned Aerial Vehicle Laser Scanning (UAVLS).

ALS emit a laser to the top of the forest canopy and collect its echoes to obtain vertical forest parameters, such as crown width, TH, and canopy structure [11]–[14]. Miłosz Mielcarek *et al.* [15] used the point cloud to extract TH from ALS data. The experimental result showed that the RMSE of extraction TH was 1.25m. Giannetti F *et al.* [16] used ALS data to extract the height of individual trees in the Mediterranean region. The experimental results showed that the coefficient of determination R^2 was 0.97. However, due to the occlusion between the trees, lasers have poor penetration of the trunk and branches under the canopy. As a result, the laser echo can only be partially retrieved, resulting in incomplete or largely inaccurate extracted forestry parameters [17], [18]. In addition, for forest areas with a high tree density, mutual sheltering between trees also reduces the visibility from above the canopy. Experiments showed that ALS is not suitable for below canopy forest parameter extraction [19]. The forest point cloud data collected by Dalla Corte *et al.* based on high-density ALS instruments (1400 points/m2) had a higher point density. Due to the farther scanning distance, the points density was still relatively low compared with the density provided by TLS. Therefore, ALS is not as suitable for extracting DBH as it is for TH. ALS is more suitable for the extraction of tree parameters in forests with low tree density or during the leaf-off period [20].

TLS is installed on the ground closer to the trees and return a denser forest point cloud (Greater than 10000 points/m^2), which can be used to extract DBH, height under branches, biomass, and leaf area index [21]–[23]. Reference [16] showed that using TLS data to extract DBH and the coefficient of determination R^2 was greater than 0.99. Conto *et al.* used the Hough transform to extract DBH from TLS data. The RMSE was 2.15 cm and the deviation was 1.09 cm [24]. Lindberg E *et al.* [25] used TLS data to extract the DBH of a single tree. Experimental results showed that the RMSE of DBH extracted using TLS data was 3.8 cm. In the forest, TLS cannot obtain the top point of each tree because of the spacing between each tree is small, which makes the visibility poor [26]. In addition, restricted by the scanning Angle, TLS cannot accurately obtain the information of the upper tree crown, which leads to the underestimation of the extracted TH compared with the measured TH [27]. Liu *et al.* [28] used TLS to estimate the height of trees. The RMSE of TH was 1.23m. The experimental results that the extracted TH was underestimation compared to the measured TH. TLS is not suitable for extracting TH in forest areas with high tree density. TLS is only suitable for TH extraction in the open area with good visibility effect [4].

In summary, obtaining high-precision forestry parameter requires combining the data collection from ALS and TLS [19], [29], [30]. Compared with MAVLS, UAVLS has the following advantages: (1) When equipped with the same type of LiDAR, the flying speed and altitude of the UAV are lower than that of a MAV. Therefore, the density of points scanned by UAVLS is greater than that of MAVLS; (2) Flexible and lightweight to carry; (3) Low flight cost and manufacturing cost. This article describes the extraction of TH based on the UAVLS and DBH based on TLS. In this paper, a method based on point density analysis was proposed to automatically extract DBH. First, two collected point cloud datasets are registered, so that the data are all in the same coordinate system. Then, the data obtained by UAVLS is divided into each individual tree and extracted the TH. With the proposed method, rather than segmenting the complete point cloud obtained by TLS into each individual tree, the TLS data at the breast height is sliced. All points of the slice are subdivided by the point density analysis method, and then the DBH is obtained. Finally, the estimated data are compared to field measurements to verify the accuracy of the approach.

II. MATERIALS AND METHODS

A. STUDY AREA

The first study area (Figure 1) in this paper is located in the Laohugou forest area (115°28′0.3144″ E, 40°59′13.4016″ N) in Zhangjiakou City, Hebei Province, China. Laohugou is a natural forest area with a complex environment and topography, with uneven tree growth (Figure 2). The average slope is about 30° and the average altitude is 1750 m. A rectangular sample plot of 100 m×100 m was selected as the research area. The plot is composed of two trees species, white birch (70 %) and larch (30 %). Tree growth is complex and uneven in size. The second study area (Figure 1) is located in the Saihanba forest area (117°23'50.4204″ E, 42°22'0.4044 N) in Chengde City, Hebei Province, China. Saihanba is an artificial plantation forest farm with relatively flat terrain and an average elevation of about 1700 m (Figure 3). A 40 m×40 m mixed forest rectangular plot, mainly composed of larch and white birch was selected as the research area.

We did not measure the TH and DBH of all the trees in the two forest areas because limited by the labor cost of field measurement. The sample plot area in Laohugou forest area is 1 hectare and the natural growth of trees is relatively complicated (due to natural growth and no artificial planning, the growth structure of natural forest trees is not as regular as the artificial forest), We cut a 25m×25m sample plot from the

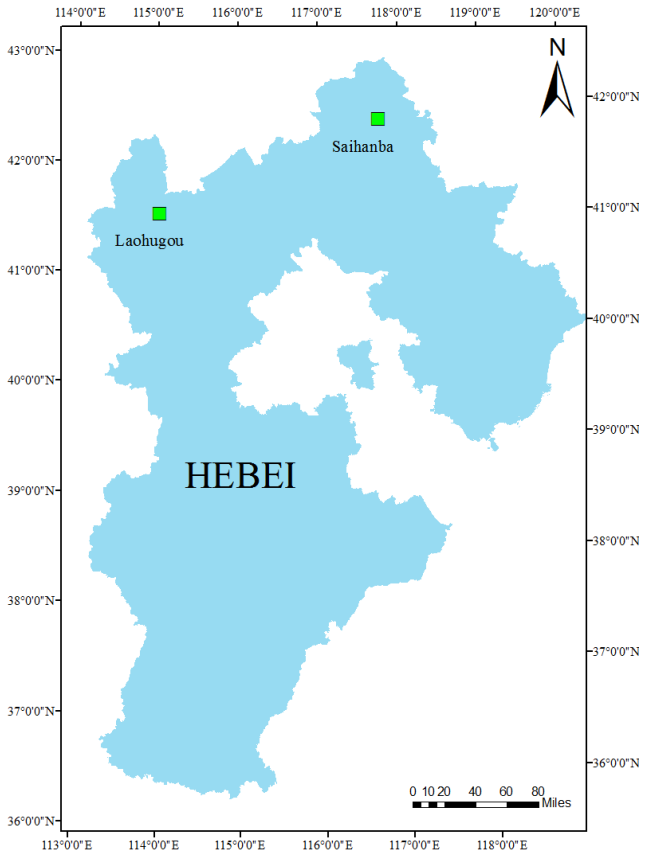

FIGURE 1. The location map of the study area.

FIGURE 2. Environment of Laohugou forest area.

Laohugou forest area and measured the TH and DBH of all trees in this sample plot (8 trees of larch and 13 trees of white birch). Due to artificial planting interference, the growth status of the same tree species is regular, and the change between each tree is small. We measured tree height and DBH of all trees (10 trees of larch and 10 trees of white birch) in 20m×20m sample plot that divided from Saihanba forest area. TH was measured by the Laser rangefinder (the model is DELIXI ELXCTRIC and the measuring accuracy is 0.1m) and DBH was measured by the Tree diameter measuring ruler. This is also the most commonly used measurement tool for measuring these two kinds of parameters in forestry.

FIGURE 3. Environment of Saihanba forest area.

B. DATA COLLECTION

1) UAVLS DATA

The UAVLS data was collected by Beijing SureStar R-Fans-16 LiDAR. The UAV set the strip width to 200 m to obtain a larger range of sample data. The flying altitude was set to 80 m to obtain fine point cloud data while ensuring flight safety. Other parameter settings are shown in Table 1.

TABLE 1. UAV LiDAR parameters settings.

Instrument parameter	Beijing SureStar R-Fans-16 LiDAR
Flight strip width	200m
Flying height	80m
Flying speed	3m/s
Laser wavelength	905nm
Maximum pulse frequency	320kHz
Angle measurement resolution	2°
Point density	270points/m^2

2) TLS DATA

Due to the large differences in the environments and the growth of trees between the two plots, different ground-based LiDAR instruments were used for data collection. In the Laohugou forest area, we used an instrument with higher scanning point density (Faro F350). The refined scan prepared the data for the subsequent extraction parameter. Due to the large forest area of the sample plot and the severe occlusion between trees, we needed to obtain the full-view point cloud of the tree trunk to extract the DBH. Therefore, a total of 38 stations (Figure 4-a) were set up for the plot scan. The distance between every adjacent station was 15-20 m. Other parameter settings are shown in Table 2.

TABLE 2. Faro such as instrument parameters setting.

Instrument parameter	Faro F350
Measuring point density	976000 points/s
Horizontal angle	0-360°
Vertical angle	30-130°
Resolution	1/4
Maximum measuring distance	350m
Laser wavelength	1550nm

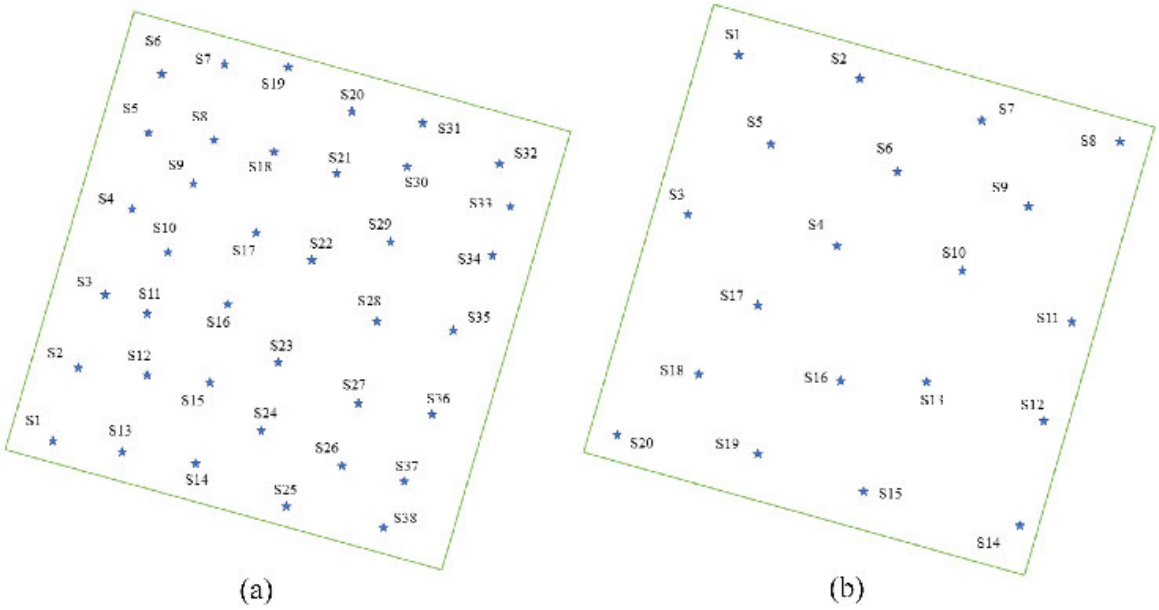

FIGURE 4. TLS instrument erection site map: (a) Laohugou forest area; (b) Saihanba forest area.

TABLE 3. Riegl VZ-1000 such as instrument parameters setting.

Instrument parameter	Riegl VZ-1000
Measuring point density	300000 points/s
Horizontal angle	0-360°
Vertical angle	30-130°
Resolution	0.06°
Maximum measuring distance	450m
Laser wavelength	1550nm

For the Saihanba forest area, we used the Riegl VZ-1000 with relatively fast scanning speed was used for data collection. A total of 20 stations (Figure 4-b) were set up for the mixed forest plots and the distance between each station was 15-22 m. Other parameter settings are shown in Table 3.

C. DATA PREPROCESSING

1) POINT CLOUD REGISTRATION

The two sets of UAVLS data were collected under the same coordinate system and fused. The point cloud data collected in this way are relatively dense, which is convenient for parameter extraction. For the point cloud data obtained by Faro F350 Terrestrial LiDAR, we used FARO RevEng Capture to search for the target ball with the same location in two adjacent stations for stitching the data; the average error was 0.0073m. For the data obtained from the Riegl VZ-1000, RiScan Pro was used to search the target slices of the same name at adjacent stations. The number of search target slices with the same name in two adjacent stations should be at least three. The point cloud attachment was carried out according to the target slices of the same name at two adjacent stations; the average error after splicing was 0.007 m. In this way, the point cloud data of all stations were in the same coordinate system. The TLS data and the USVLS data were coarsely registered using human-computer interaction. The details were as follows: (1) We used Global Positioning System (GPS) receivers to measure the boundary of each plot (the Laohugou plot obtains the position of each pillar point; the Saihanba plot obtains the position of the small flag intersection); (2) We used the CloudCompare software to match the boundary information in the TLS data with the boundary position information collected by the GPS receiver (Figure 5). And then the Iterative Closest Point (ICP) algorithm [20] was used for fine registration to ensure that the TLS data and the UAVLS data were in the same coordinate system (Figure 6). The UAVLS data and TLS data accurate fusion can ensure that the extracted TH and DBH automatically match the same tree based on location.

FIGURE 5. The boundary position information of the sample plot was collected by the GPS receiver.

2) NOISEL REMOVAL

LiDAR data is affected by the external environment and working mechanism, which produces noise and outliers in

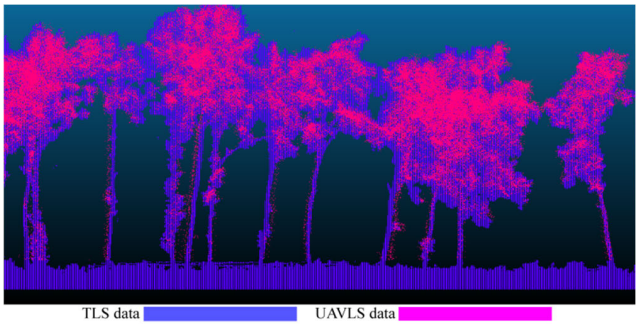

FIGURE 6. TLS and UAVLS data fusion.

the collected data. These noise points cause errors in the extraction of forestry parameter. Therefore, the data needs to be denoised before extracting the structural parameter. The gradient filter algorithm [31] was used for denoising because the point cloud density obtained by UAVLS was relatively low. The point cloud density obtained by TLS was relatively large and the scan data was relatively fine, causing outliers and noise points to be scattered, so a statistical filtering algorithm [32] was used for denoising.

3) GROUND POINT SEPARATION

During LiDAR data collection, weeds, low shrubs, and ground are also scanned. These objects are collectively called ground points. The existence of ground points affects the accuracy of canopy parameters extraction, so they need to be separated. In this study, we separated the ground points using the Cloth Simulation Filter (CSF) [33]. The algorithm is based on the idea of using a cloth falling under gravity to obtain a physical representation of the terrain. This method has fewer parameters and faster separation than other methods.

4) SINGLE TREE SEGMENTATION

There are many research methods for single tree segmentation from LiDAR data [34]–[37], and most of them are classified into either canopy height model (CHM) or point cloud algorithms. The CHM-based method mainly uses the existing image segmentation technology and region growth technology to generate a raster image on the surface of the LiDAR data and then extract every single tree. Based on the idea of point cloud clustering single-tree segmentation, the three-dimensional point cloud data is segmented directly, limiting information loss. To increase the accuracy of the single tree segmentation, we used two segmentation methods (based on CHM and point cloud) to extract individual trees separately. The point cloud data of every single tree segmented by these two methods were compared. The single tree point cloud with complete segmentation was selected to represent the point cloud of this tree. We used a human-computer interaction method (trees with cross crowns or under-divided single trees need to be manually divided) to correct unsatisfactory tree segmentations.

D. RESEARCH METHODS

In this research, we combined UAVLS and TLS data to extract forestry parameter with higher accuracy. UAVLS data was used to extract TH, while TLS data was used to extract DBH. The method proposed in this paper can obtain higher TH extraction accuracy and automatic extraction of DBH. The workflow of this process is shown in Figure 7. We pre-processed the acquired UAVLS and TLS data to generate the DEM and then used it to normalize the combined point cloud. We segmented the forest point cloud data obtained by UAVLS into individual trees. The TH was extracted from the segmented single tree point cloud data. We sliced the data obtained by TLS at the height of the breast diameter. Then, our proposed point density analysis method was used to automatically extract the DBH. The DBH of the TLS data was no longer required for single tree segmentation.

1) TH CALCULATION

In forestry, TH is defined as the vertical distance from the highest point of the tree to the ground. Because the data was normalized before dividing the UAVLS data, the lowest point of all point cloud data is the height Z equal to 0. After the single tree division, we obtained the highest point $Z_{i^{max}}$ and lowest point $Z_{i^{min}}$ of each tree from the UAVLS data to extract the height of a single tree. The formula for tree height H_i is as follows:

$$H_i = Z_{i^{max}} - Z_{i^{min}} \tag{1}$$

where i represents the tree number.

2) DBH EXTRACTION MODEL

For the extraction of DBH, this paper did not perform a single tree segmentation on the TLS data for three reasons: First, the point density of TLS is relatively high, the amount of data is much larger than that of UAVLS, and the segmentation speed is slow when single tree segmentation is performed; Second, the distribution of point density obtained by multi-site cloud scanning for each tree trunk is not uniform, which affects the results of single tree segmentation and DBH extraction; Third, we only need to obtain the section at a height of 1.3 m from the ground for the extraction of the DBH and the subsequent measurement. Therefore, we cut the TLS data at a height of 1.3 m from the ground by 4 cm and extracted the DBH by segmenting the slice (Figure 8-a).

In this paper, an improved K-means algorithm was introduced to further eliminate noise points and outliers. The K-means algorithm is a clustering algorithm based on the Euclidean distance. Points closer to the seed point are more likely to belong to the same type. The seed points in the traditional K-means algorithm are randomly generated. Since the seed points are irregularly distributed, the point used to calculate DBH will be clustered within the range of other seed points. Therefore, the grid projection was used to calculate the number of projection points within each grid. The points where the DBH is cut are relatively concentrated and the seed points are generated in areas with higher point density, and

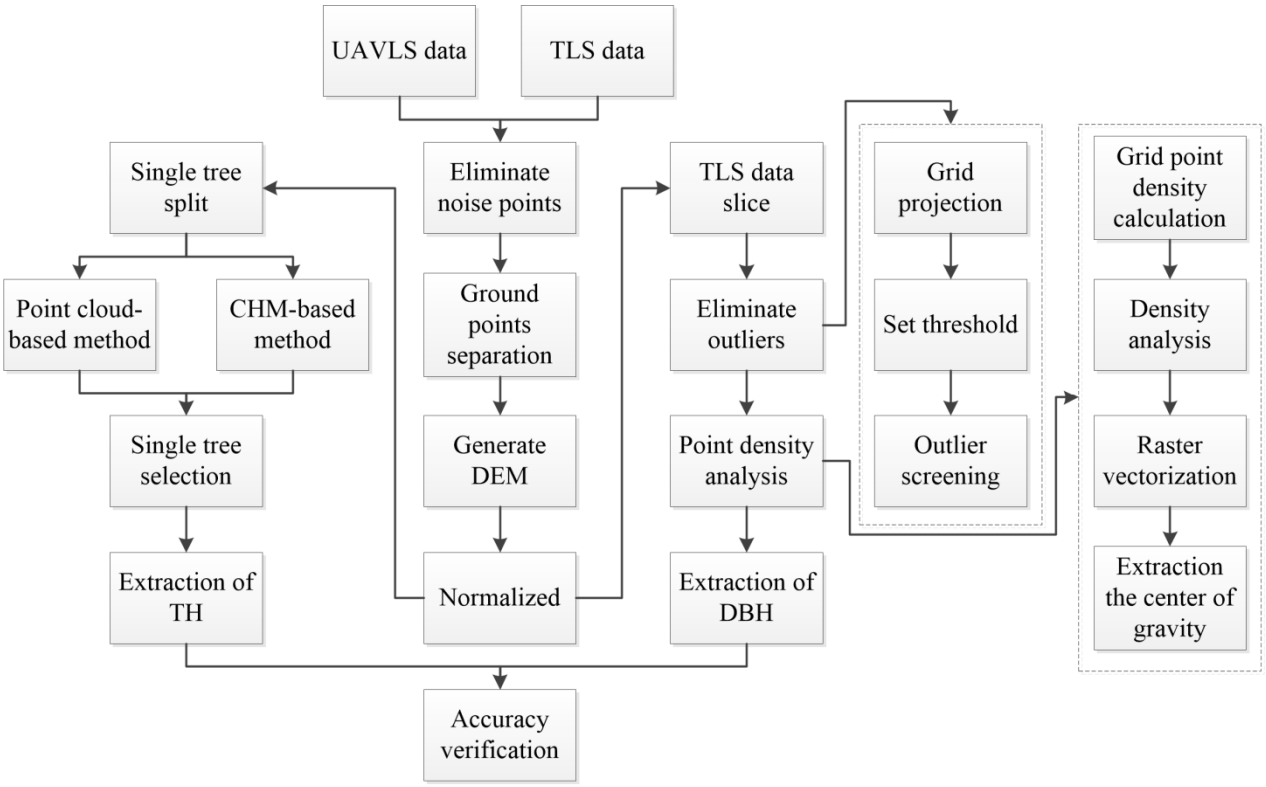

FIGURE 7. Workflow of forest parameter extraction.

thus they will be located around the DBH. We calculated the point density U in each grid, then set the point density threshold V, and the number of U greater than V as the K value. The seed point set was as M, and the various sub-points as m:

$$M = \{m_1, m_2, m_3 \cdots m_k\} \tag{2}$$

We used the maximum stem diameter to limit the growth area of each seed point to realize the unsupervised clustering of points, and roughly eliminate outliers and noise points caused by slicing (Figure 8-b). Those branch point clouds that are difficult to be eliminated, which are processed by manual editing (Figure 9). Next, every single DBH will be extracted and measured. Finally, the point density analysis method was used to extract the DBH, following these steps:

(1) The point cloud data was performed point density analysis after removing the outliers, and calculated the point density formula around each raster pixel (grid):

$$P = \frac{N}{S} \tag{3}$$

where P is the density, N is the total number of points, and S is the pixel area;

(2) We extracted the denser area as the grid area where the stems were located;

(3) The extracted grid area was collected for point sets, and the collection of adjacent points was extracted from the top to the bottom or from the left to the right. We constructed polygons based on the extracted points, starting the search downward in boundary order with a node as the starting point, connecting the next node to form an external polygon, establishing a topological relationship, and then determining whether each polygon contained or connected to obtain a vector graphic;

(4) The obtained vector polygon was used to find its center of gravity to replace the position of the polygon and then the position of the tree DBH. The formula is as follows:

$$x = \frac{\sum_{i=2}^{n-1}(x_1 + x_i + x_{i+1}) \begin{bmatrix} x_1 & y_1 & 1 \\ x_i & y_i & 1 \\ x_{i+1} & y_{i+1} & 1 \end{bmatrix}}{3\sum_{i=2}^{n-1} \begin{bmatrix} x_1 & y_1 & 1 \\ x_i & y_i & 1 \\ x_{i+1} & y_{i+1} & 1 \end{bmatrix}} \tag{4}$$

$$y = \frac{\sum_{i=2}^{n-1}(y_1 + y_i + y_{i+1}) \begin{bmatrix} x_1 & y_1 & 1 \\ x_i & y_i & 1 \\ x_{i+1} & y_{i+1} & 1 \end{bmatrix}}{3\sum_{i=2}^{n-1} \begin{bmatrix} x_1 & y_1 & 1 \\ x_i & y_i & 1 \\ x_{i+1} & y_{i+1} & 1 \end{bmatrix}} \tag{5}$$

where x_i and y_i are divided into the coordinates of the vertices of the polygon, n is the total number of vertices, i is a lower bound on the number of vertices.

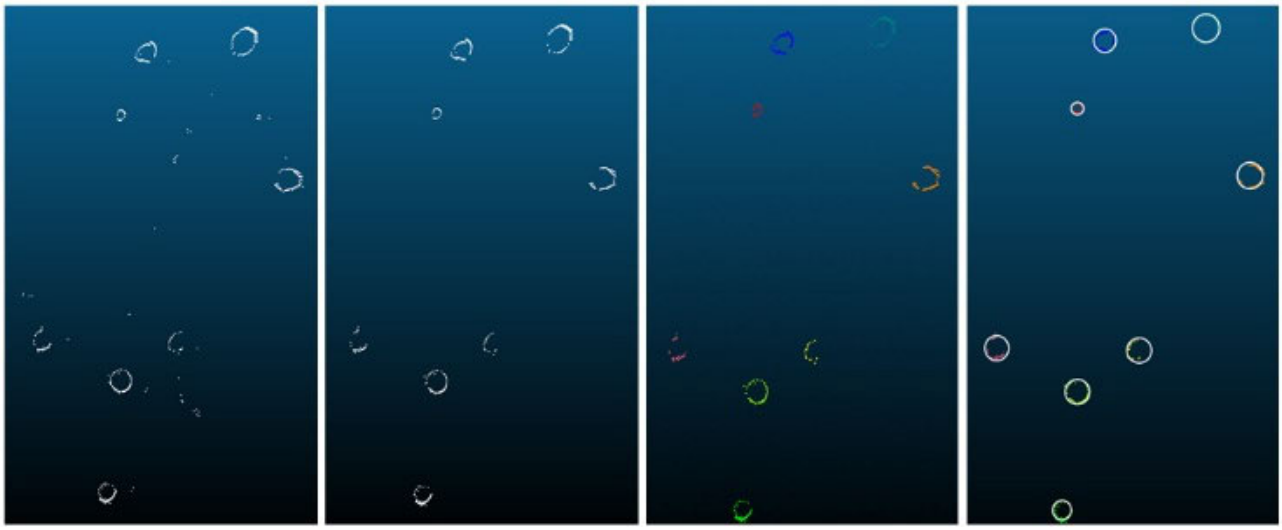

FIGURE 8. DBH slices of a sample of the data: (a) the original slice point cloud; (b) the improved k-means algorithm was used to eliminate the slice point cloud after outliers; (c) tree trunk point cloud slice extraction; (d) fitting diagram of DBH.

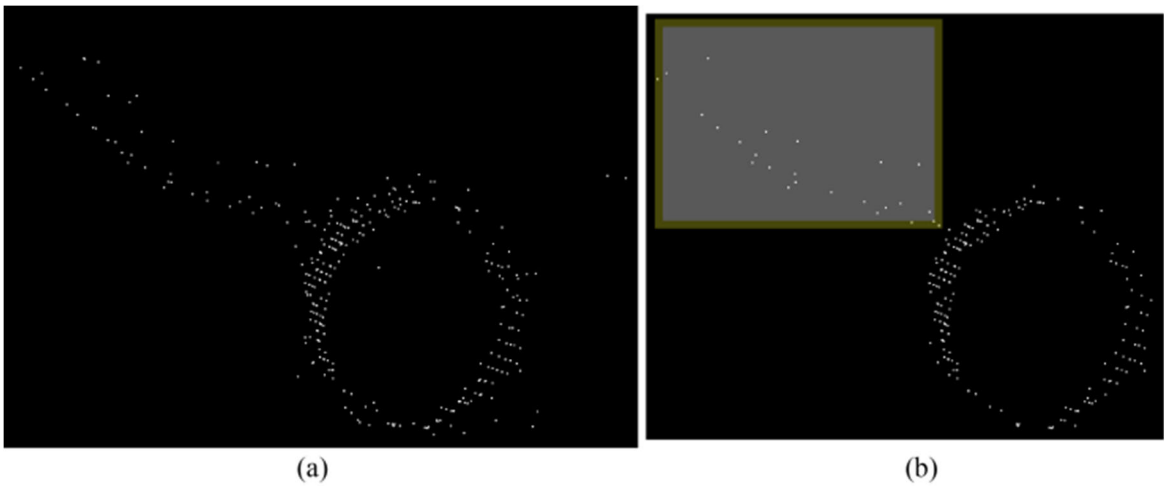

FIGURE 9. Tree trunk point cloud slicing: (a) the original slice point cloud; (b) the point cloud slices after denoising.

(5) We searched for the closest point according to the determined point of DBH using the formula:

$$d_{min} = \sqrt{(m_p - m_{p+1})^2 + (n_p - n_{p+1})^2} \tag{6}$$

where (m, n) is the position of each stem center; d_{min} is the shortest distance between DBH.

(6) The DBH of each stem was extracted (Figure 8-c).

3) DBH CALCULATION

The extracted DBH data were projected on the x-y plane so that there were some discrete points on the plane. These discrete points show a top view, which is the best observation angle for the DBH. Therefore, the discrete points were fitted to find the DBH. We then eliminated the large discrete points with larger influence to ensure more accurate fitting accuracy. First, we roughly estimated the position of the center of each stem, finding the average x- and y- value among all the points, according to:

$$x_m = \frac{\sum_{i=1}^{n} x_i}{n} \tag{7}$$

$$y_m = \frac{\sum_{i=1}^{n} y_i}{n} \tag{8}$$

$$d_i = \sqrt{(x_m - x_i)^2 + (y_m - y_i)^2} \tag{9}$$

The point (x_m, y_m) was used as the center to find the distance d_i from each discrete point to this point. We used box plots to distribute the discrete data to calculate the quartiles of the d_i set, calculated as follows:

$$Q_1 = \frac{(n+1)}{4} \tag{10}$$

$$Q_2 = \frac{(n+1)}{2} \tag{11}$$

$$Q_3 = \frac{3(n+1)}{4} \tag{12}$$

We sorted d_i from small to large, and took the discrete points between positions Q_1 and Q_3 as the fitting data, which eliminated the influence of gross error points on the fitting.

After that, we used a general and classic least squares method for fitting [38]. The circle was defined as follows:

$$(x - x_c)^2 + (y - y_c)^2 = R^2 \tag{13}$$

To fit a circle with least-squares, we minimize the sum of squares of the distance, as:

$$D_{min} = \sum (\sqrt{(x_i - x_c)^2 + (y_i - y_c)^2} - R)^2 \tag{14}$$

where x_i and y_i represent the coordinates of any point on the fitted circle, x_c and $y_c$represent the center of the circle, and R represents the radius (Figure 8-d).

4) STATISTICAL ANALYSIS

To evaluate the accuracy of the TH and DBH obtained by the LiDAR data against manual measurements, we used the coefficient of determination (R^2), the RMSE, and the mean absolute error (MAE). R^2 was calculated as:

$$R^2 = 1 - \frac{\sum_{i=1}^{n} (P_i - Q_i)^2}{\sum_{i=1}^{n} (P_i - Q_{mean})^2} \tag{15}$$

where n represents the number of verification samples, P_i is the estimated value, Q_i is the measured value, and Q_{mean} is the measured average value. The RMSE was calculated as:

$$RMSE = \sqrt{\frac{1}{n} \sum_{i=1}^{n} (P_i - Q_i)^2} \tag{16}$$

The MAE was calculated as:

$$MAE = \frac{1}{n} \sum_{i=1}^{n} |P_i - Q_i| \tag{17}$$

The smaller the RMSE and MAE and the larger the R^2, the better the extraction effect and the higher the accuracy. We used this method to evaluate the extraction accuracy of TH and DBH in each experimental plot. We used the mean intersection over union (MIOU) to evaluate the segmentation accuracy of the DBH from the slice point cloud, calculated as follows:

$$MIOU = \frac{1}{k} \sum_{i=1}^{k} \frac{TP}{FN + FP + TP} \tag{18}$$

where k represents the number of trees, and TP represents the points predicted to be the real trunk point cloud. FP represents the point of segmentation error. TN represents that the real trunk points were predicted incorrectly.

5) METHOD IMPLEMENTATION ENVIRONMENT

This paper analyzed the use of CloudCompare software to preprocess LiDAR data. Using C++ and Python programming language to achieve single tree segmentation, TH extraction, improved K-means algorithm, automatic DBH segmentation and DBH extraction.

III. RESULTS

A. TH MEASUREMENT

To verify the accuracy of TH extraction, we compared the ground measured TH with the extracted TH. For the Laohugou forest plot, the TH obtained by LiDAR ranged from 6.8 to 14.72 m and the average TH was 11.47 m. The manually-measured TH was between 6.5 and 14.7 m and the average TH was 11 m (Figure 10). The extracted average TH was 0.47 m higher than the measured average TH. The maximum error between the measured TH and the extracted TH was 1.2 m. There is a strong relationship between the manually-measured TH and the extracted TH (Table 4). We extracted the TH of larch and white birch respectively, and compared the extracted TH with the ground measured TH (Table 5). Both of the extracted average TH were higher than the ground measured TH (Figure 10). For the Saihanba forest plot, the extracted average TH was 0.6 m higher than the measured average TH. The maximum error between the manually measured TH and the extracted TH was 1.172 m. The quartiles of the extracted TH were all higher than the measured data, and the extracted TH were overall higher (Figure 10). The average and maximum error of white birch TH extraction were larger than those of larch, which were 0.64 and 1.172 m, respectively (Table 6 and Figure 10). Through the above experimental analysis, whether in the natural growing forest or in the artificial planted forest, we used the UAVLS data to extract the TH with relatively high accuracy.

TABLE 4. Accuracy assessment of TH.

Study area	R^2	RMSE (m)	MAE (m)
Laohugou	0.9458	0.7	0.61
Saihanba	0.95	0.65	0.57

TABLE 5. Laohugou study area.

Tree species	R^2	RMSE (m)	MAE (m)
larch	0.953	0.677	0.56
white birch	0.92	0.724	0.65

TABLE 6. Saihanba study area.

Tree species	R^2	RMSE (m)	MAE (m)
larch	0.97	0.56	0.51
white birch	0.88	0.72	0.63

We analyzed the extracted TH of white birch and larch on two plots. The average error of larch TH extraction was 0.11 m lower than that of white birch. The R^2 of larch was better than the white birch of R^2 (Figure 11-a and Figure 11-b). This was mainly due to not accurate measurement the top of tree. The top of the larch tree was pointed, and the apex

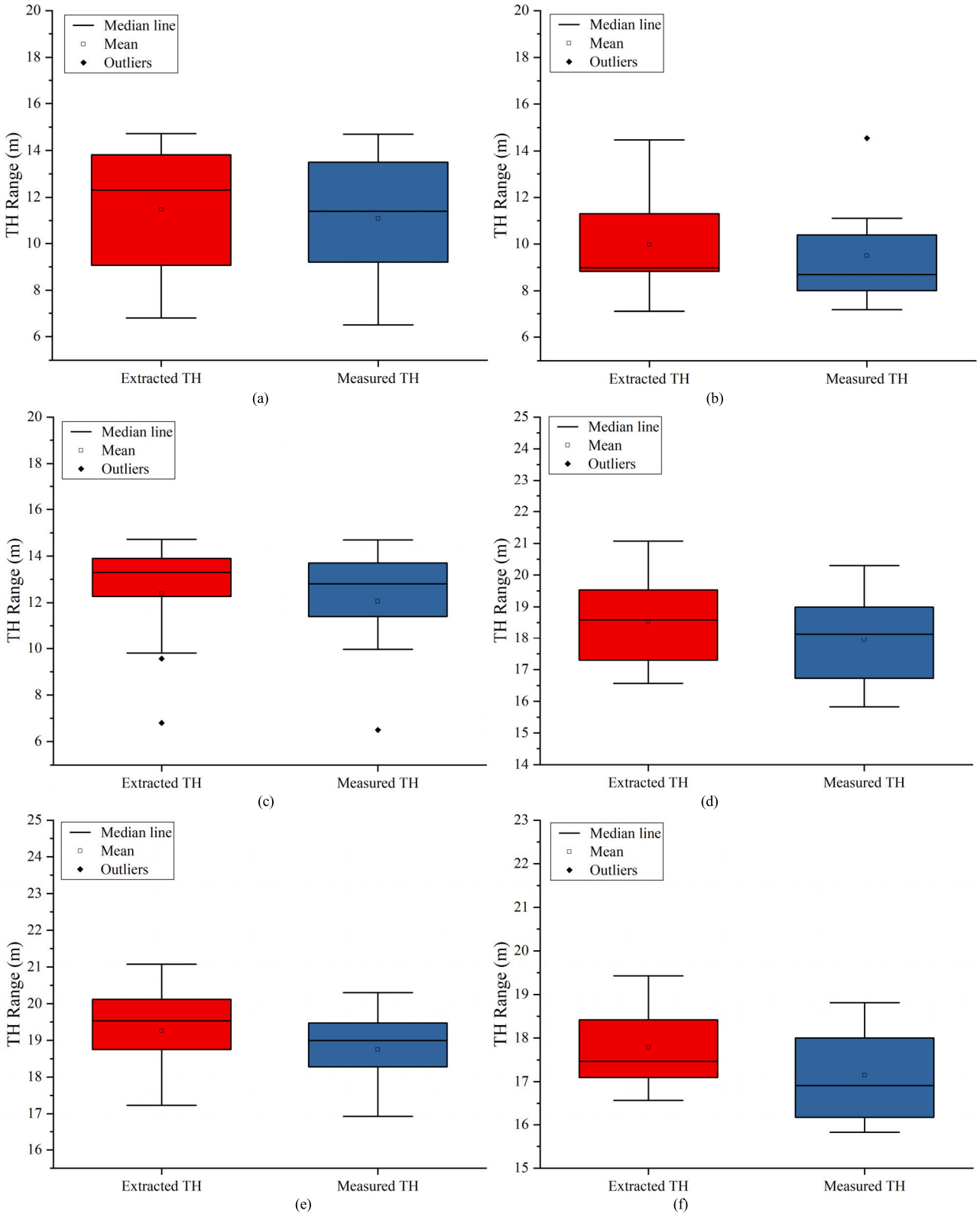

FIGURE 10. (a) Box plot of TH in Laohugou plot; (b) Box plot of larch TH in Laohugou plot; (c) Box plot of white birch TH in Laohugou plot; (d) Box plot of TH in Saihanba plot; (e) Box plot of larch TH in Saihanba plot; (f) Box plot of white birch TH in Saihanba.

of the tree was easy to be measured by the laser spot. The top of white birch was fluffy, which was prone to deviation when obtaining the apex of the tree (Figure 12). Whether it was white birch or larch, the average TH extracted was higher than the TH ground measured (Figure 11-c). On the one hand, when the TH was actually measured, the highest

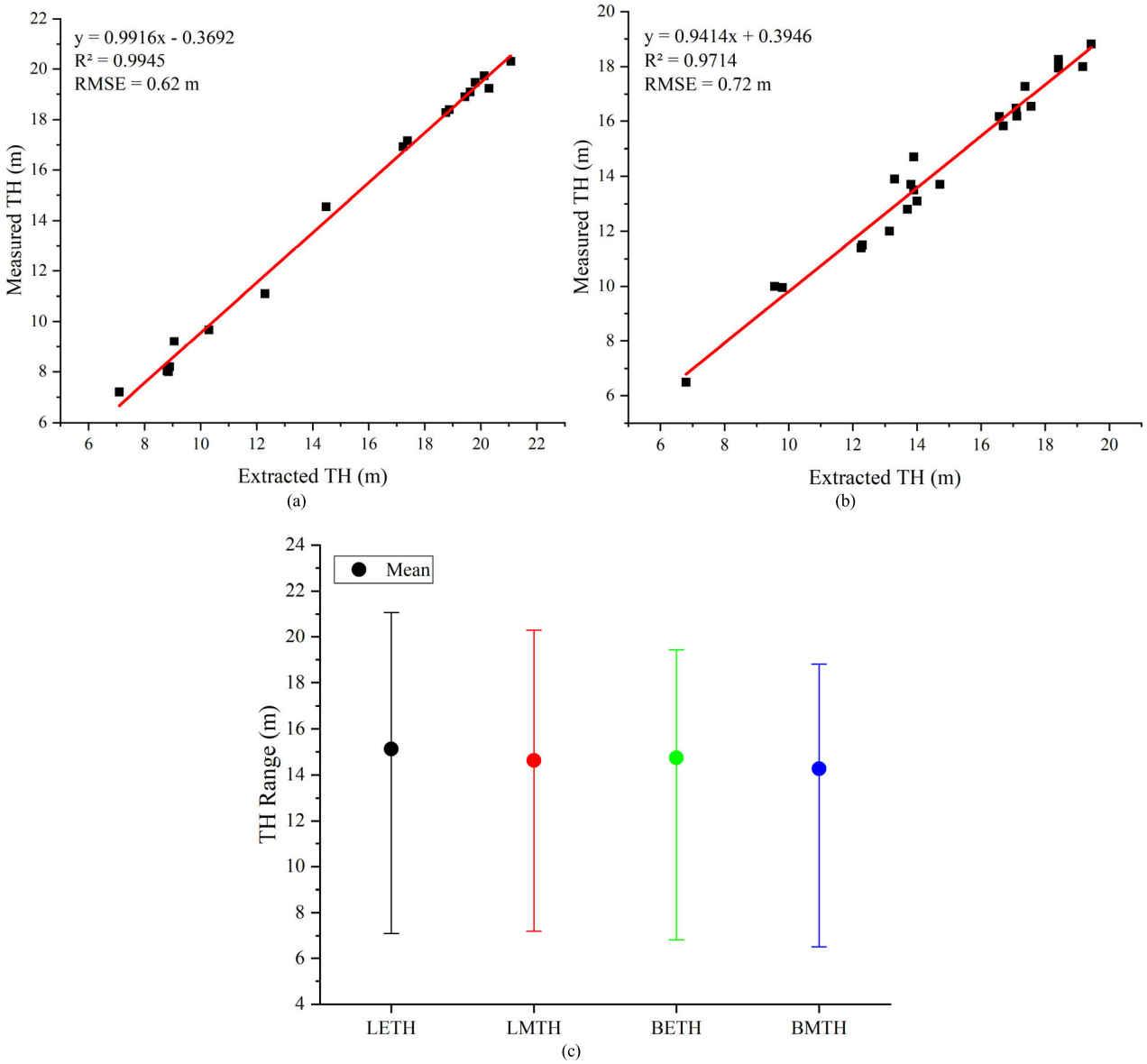

FIGURE 11. The relationship between the extracted and the measured parameters of TH at two forest plots: (a) Scatterplot of extracted vs measured larch TH; (b) Scatterplot of extracted vs measured white birch TH; (c) Distribution intervals of TH extraction and ground measurement for different species (LETH: The extracted TH of larch; LMTH: The ground measured TH of larch; BETH: The extracted TH of white birch; BMTH: The ground measured TH of white birch).

point of the tree cannot be obtained due to the occlusion between the canopy, which causes the actual measurement error. On the other hand, the parameter settings of ground point filtering and UAVLS data height normalization will also affect the accuracy of the extraction TH. The ground points were not completely separated, and the DEM result generated according to the ground points was lower. After that, the generated DEM was used to normalize the UAVLS data, which causes the CHM result greater than the true value, and then the extracted TH was on the high side.

B. DBH EXTRACTION

Our method of extracting the DBH was to slice 4 cm thick layers of points at the height of 1.3 m. After that, the whole slice was automatically divided into the DBH. The number and completeness of the slice point cloud at the height of breast diameter were extracted by means of human-computer interaction as a benchmark. In the Laohugou forest area, our extraction method over-segmented the data. We used MIOU to evaluate the segmentation accuracy of the tree trunk point cloud slices in each forest sample plot. We measured 21 trees in the Laohugou forest area and extracted 23 tree trunk slice point clouds. The MIOU extracted by our method from the point cloud section of the trunk in Laohugou forest area was 0.86. In the Saihanba forest area, the extraction accuracy of our method reached 100%. In the Saihanba forest area, we manually measured 20 trees and extracted 20 tree trunk slice point clouds. The MIOU extracted from the

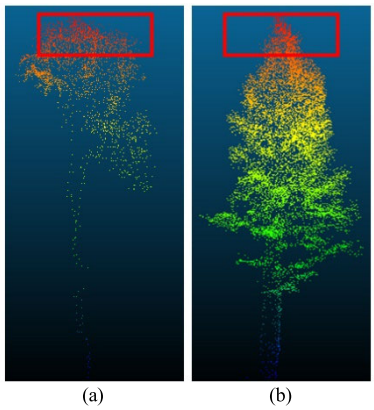

FIGURE 12. The tree top of white birch (a) and larch (b).

tree trunk point cloud slices in the Saihanba forest area was 0.92(Figure 13).

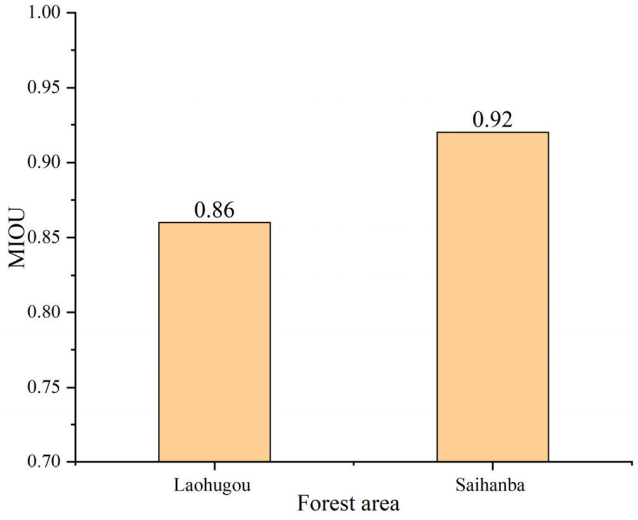

FIGURE 13. Extracted tree trunk section MIOU.

C. DBH MEASUREMENT

This paper compared the extracted DBH with the measured DBH to evaluate the accuracy of DBH extraction. In the Laohugou forest area, the extracted DBH ranged from 6.38 to 29.41 cm, and the average DBH was 17.4 cm. The range of measured DBH was 6.36 to 30.1 cm, with an average length of 17.52 cm (Figure 14). The extracted average DBH was 0.12 cm short than the measured average DBH. The maximum error between the measured and extracted DBH was 1.23 cm. For the Laohugou forest plot, the extracted DBH was similar to the measured DBH, indicating that our method was effective (Table 7). This shows that the fitting was excellent and the measured DBH were highly correlated with the extracted DBH (Table 7). For larch and white birch, the average error of DBH extracted by our method were 0.56 cm and 0.59 cm, respectively (Table 8). The range of DBH extracted at Saihanba forest area was 19.7 to 31.84 cm and the average length of DBH was 26 cm. The DBH of the Saihanba forest area sample obtained by manual measurement ranged from 18.9 to 31.97 cm and the average length was 26.1 cm (Figure 14). The maximum error between the extracted DBH and the measured DBH was 0.79 cm. The measured DBH of the Saihanba forest plot were similar to the median of the extracted DBH, reflecting the overall closeness between the measured DBH and the extracted DBH, indicating the feasibility of the DBH extraction method (Figure 14). The extracted and measured DBH of the Saihanba forest plot were also linearly fitted, which further reflected the closeness between the extracted and the measured DBH (Table 7). Our DBH extraction method was, therefore, extremely effective and accurate. The average error of the DBH of the two species of larch and white birch were similar, 0.34 cm and 0.41cm, respectively (Table 9). The DBH extracted from the point cloud and the ground measured DBH of each tree species reached a very high degree of linear fit ($R^2 > 0.95$) (Table 9).

TABLE 7. Accuracy assessment of DBH.

Study area	R^2	RMSE (cm)	MAE (cm)
Laohugou	0.9941	0.65	0.58
Saihanba	0.99	0.43	0.38

TABLE 8. Laohugou study area.

Tree species	R^2	RMSE (cm)	MAE (cm)
larch	0.9946	0.584	0.565
white birch	0.9924	0.69	0.59

TABLE 9. Saihanba study area.

Tree species	R^2	RMSE (cm)	MAE (cm)
larch	0.9895	0.42	0.34
white birch	0.95	0.44	0.41

In this study, DBH of two different tree species from two plots were extracted separately. The statistical test confirmed that there was no statistically significant difference between DBH measured from the field and TLS data. The linear regression indicated a high R^2 of 0.9965 for larch (Figure 15-a). The linear regression indicated a high R^2 of 0.9931 for white birch (Figure 15-b). Using the TLS data to extracted DBH had minor over and underestimation compared with individual tree stem measurements (Figure 15-c). The extraction accuracy of white birch DBH was slightly lower than that of larch. The maximum error of white birch was 1.23 cm. The error mainly came from two aspects. First, compared with the larch trunk, the white birch trunk had a certain degree of curvature, and the bark was relatively soft and swollen. After the trunk was sliced, it was difficult to fit due to the shape of the slice. Second, when using TLS to obtain data, it was blocked by understory vegetation and

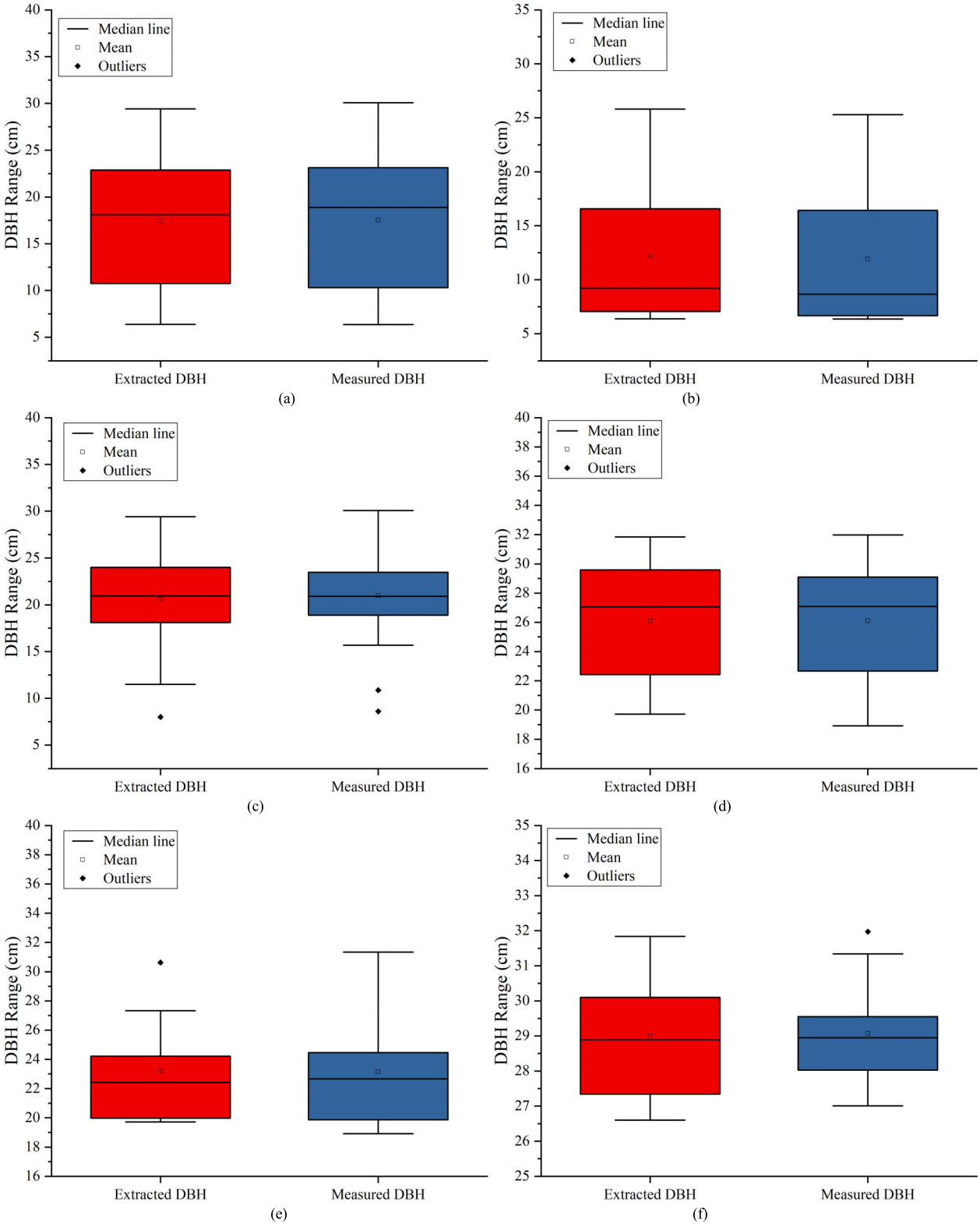

FIGURE 14. (a) Box plot of DBH in Laohugou plot; (b) Box plot of larch DBH in Laohugou plot; (c) Box plot of white birch DBH in Laohugou plot; (d) Box plot of DBH in Saihanba plot; (e) Box plot of larch DBH in Saihanba plot; (f) Box plot of white birch DBH in Saihanba.

tree trunks, making the data missing. It was more difficult to fit DBH of the missing slices. The automatic extraction and fitting method of DBH proposed by us was suitable for accurate extraction of DBH of different forest areas (natural forest and artificial forest) and different tree species (larch and white birch).

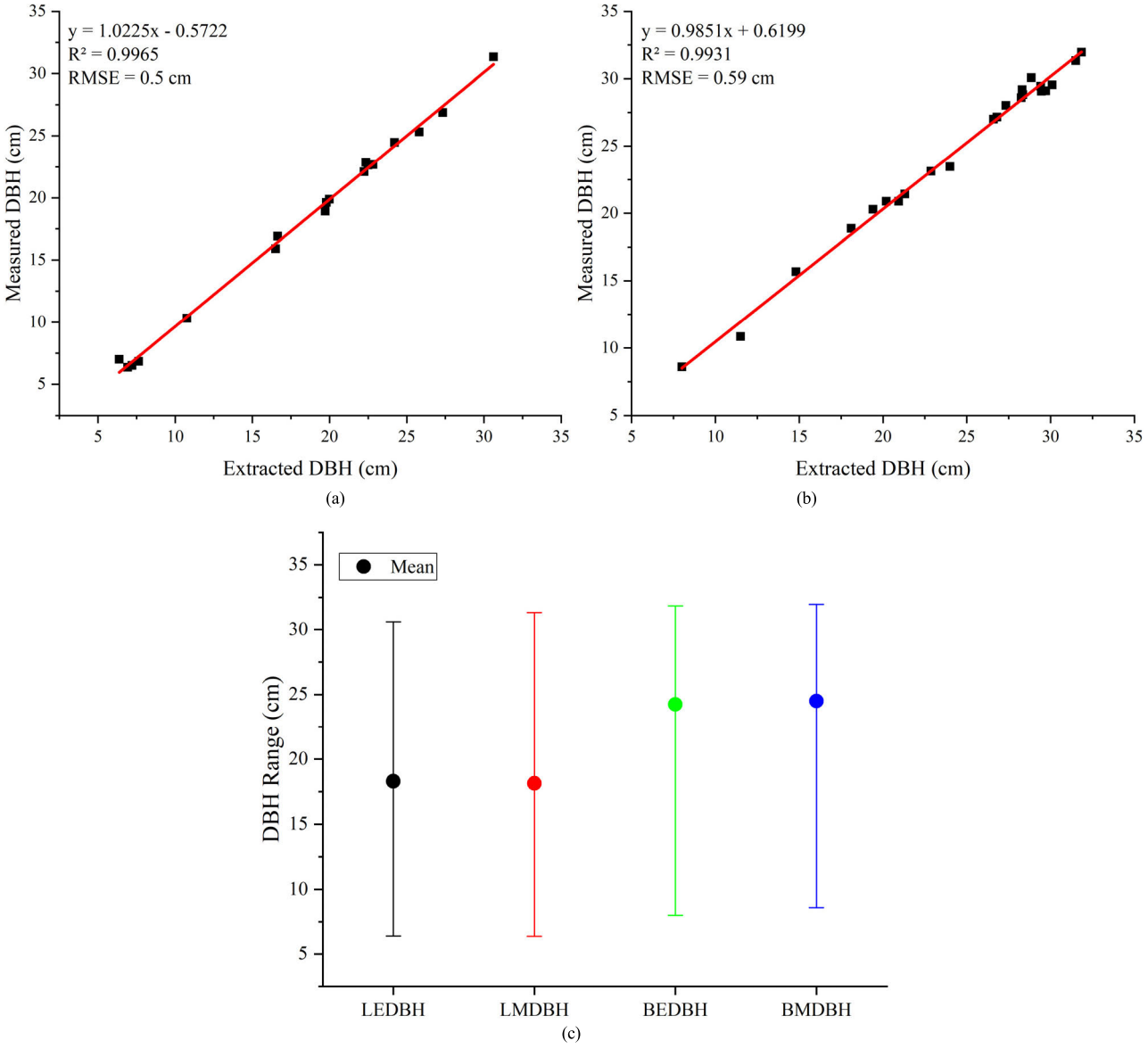

FIGURE 15. The relationship between the extracted and the measured parameters of DBH at two forest plots: (a) Scatterplot of extracted vs measured larch DBH; (b) Scatterplot of extracted vs measured white birch DBH; (c) Distribution intervals of DBH extraction and ground measurement for different species (LEDBH: The extracted DBH of larch; LMDBH: The ground measured DBH of larch; BEDBH: The extracted DBH of white birch; BMDBH: The ground measured DBH of white birch).

IV. DISCUSSION

The combination of ALS and TLS can extract high-precision forestry parameters from different platforms. Bazezew *et al.* used ALS and TLS to accurately estimate the above-ground biomass of tropical forests in Malaysia. Experimental results showed that the RMSE of upper canopy TH was 3.24 m (20.18%), the RMSE of low canopy TH was 1.45 m (14.77%) and the RMSE of tree trunk DBH is 1.30 cm (6.52%) [29]. Ye *et al.* improved the stem mapping and DBH method based on TLS data. The experimental results showed that the least-squares ellipse fitting method is more suitable for the estimation of DBH. Compared with other methods, the estimation accuracy of DBH of this method was improved, with the RMSE of 1.14 cm [30]. Wu *et al.* [19] used a combination of ALS and TLS to manage fruit tree structure, number of trees, diseases, fertilization, etc. Because of ALS's limitations in measuring branches and canopy structure from above the canopy, this technology always underestimates the canopy volume compared to field measurements. Although the above studies obtain forestry parameters from LiDAR on different platforms, they had the disadvantages of complex extraction of forestry parameters, low accuracy, and single test area.

This paper used TLS and UAVLS data to extract DBH and TH in two forest areas. To overcome interference factors such as tree occlusion that affect the accuracy of the extraction, the two data collection platforms can complement each

other's deficiencies. For complex natural forests, we only need to select the instrument erection site when the data is obtained by TLS, and perform data splicing after the data is scanned. After that, the DBH is automatically extracted by the point density analysis algorithm proposed in this paper. However, the manually measured DBH needs to be measured at the position of each tree, which increases labor costs. Although there were many researches using LiDAR for forest parameter extraction, as far as we know, there were not much studies on the combination of UAVLS and TLS for high-precision tree structure parameter extraction in natural forests and artificial forest. The UAV LiDAR acquisition platform is easy to carry, its hardware manufacturing and data acquisition costs are low, and it can be widely promoted. At present, some scholars used UAV high-density LiDAR for forestry parameter extraction research [39], [40]. However, in complex natural forest areas and dense forest areas, it is difficult for the laser to penetrate into the lower canopy completely. And it is impossible to completely extract the parameters of the trees in the lower canopy. The backpack-type LiDAR (fast data collection speed) is also used to collect data from the lower canopy (applicable to artificial forest areas), there are still two shortcomings in data collection in natural forest areas: (1) Laser spot density and ranging (100 m) lower than the TLS; (2) When collecting data, workers need to travel through the entire forest area, which consumes a lot of physical strength. For some locations in the natural forest area cannot be reached or dangerous, the backpack LiDAR cannot get the complete data of the area.

In the process of collecting data, we discovered the following problems that affect data quality. When acquiring UAVLS data, we believe that the design of flight altitude, flight speed, and route planning will all affect the data quality. When using TLS to acquire data, the choice of station location of the instrument directly affects the integrity of data acquisition. Although two different types of TLS (phased: Faro F350; pulsed: Riegl VZ-1000) were used to acquire ground point cloud data, the average distance we set up adjacent instrument stations was around 20 m and this distance was well below the maximum TLS range. The Faro F350 and Riegl VZ-1000 have a measuring precision of 1 mm and 5 mm respectively. The measurement precision errors of both instruments meet the requirements of this paper for measuring point cloud data accuracy. The selection of points with the common in the forest area will affect the fusion of UAVLS data and TLS data. We evaluated the accuracy of the extracted TH and DBH with manual measurements and found that the overall accuracy of TH is relatively high and that the extracted DBH is close to the measured DBH.

UAVLS obtains forestry data from the top to the bottom of the canopy, which can comprehensively capture the upper portion of each tree, accurately locating the position of each tree and avoiding the problems arising from tree occlusion. We also found that the TH extracted from the Laohugou forest plot (natural growth forest area) and the Saihanba forest plot (artificial planting forest area) were both larger than the field measurement. We concluded that the TH error mainly derived from two aspects. First, TH was manually measured with a laser rangefinder that obtained the top and bottom of the tree. Due to the occlusion within canopies, the laser rangefinder was unable to obtain the exact treetops. This caused the manually-measured TH to be too small. Second, in forest plots, the method of measuring TH by felling trees is unrealistic. Sibona *et al.* [41] measured the TH of felled trees in the field and found that they were lower than the TH extracted from LiDAR data. Stereńczak *et al.* [42] also pointed out that there are errors in field measurements of TH. This also further demonstrated that the extracted TH is higher than the field measured TH. Research by Thomas Hilker *et al.* [43] showed that the average TH extracted by ALS was higher than other measurement methods. In addition to the above-mentioned factors that affect the accuracy of the LiDAR data, the noise points of the LiDAR data, the parameter settings during the single tree segmentation, the influence of the canopy and the terrain are also important factors that affect the accuracy [44]–[46]. We also analyzed the extracted TH of different tree species in the two plots. The extraction accuracy of larch was slightly higher than that of white birch. The main reason was that the outlines of the trees were great different, and the treetop of the larch tree was easier to obtain than the white birch. In addition, the crown shape of white birch is fluffy. Pseudo-treetop may be extracted when performing single tree segmentation, resulting in single tree point cloud over-segmentation and inability to extract TH accurately.

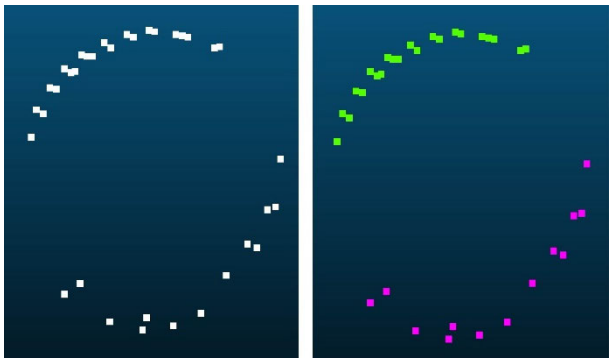

FIGURE 16. Over-segmentation of the tree trunk point cloud slice.

We used the data collected by TLS to extract the DBH. In earlier studies, it was necessary to segment all the trees in the entire study area [30], [47], [48]. Due to the large amount of TLS points, low efficiency and high computational costs may occur when single tree segmentation is performed. In response to the above problems, some studies proposed to slice the data to overcome the need to perform single tree segmentation [28]. We also sliced all the trees and segmented each tree by automatically extracting DBH. In the Laohugou forest area, the slices of the tree trunk point cloud at DBH were over-segmented. We analyzed three sources of error. First, the tree trunk point cloud scan was incomplete

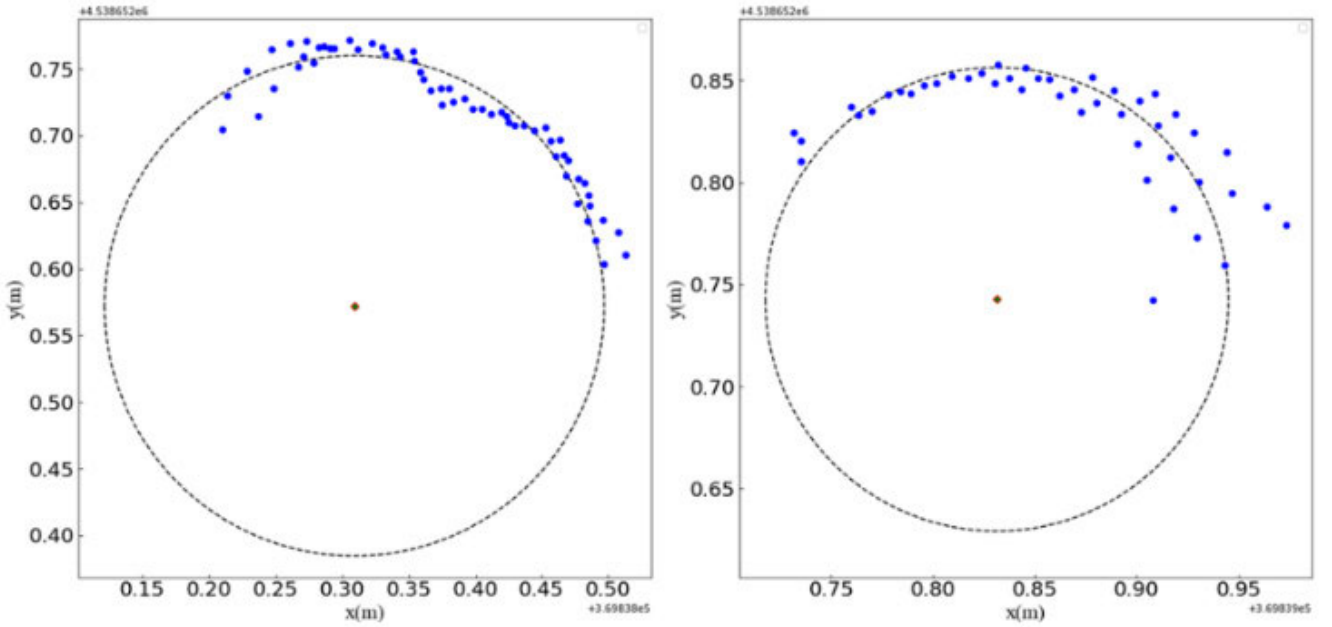

FIGURE 17. DBH with incomplete data fitting.

due to mutual occlusion between trees. Because the sliced point cloud data was incomplete, it was divided into two or more parts during the extraction (Figure 16). Second, when we used the improved K-means algorithm to eliminate the branch points, the parameter setting was too large to eliminate the tree trunk point cloud, resulting in incomplete slices. Third, the parameter settings of point density analysis and grid grading also affected the extraction of trunk point cloud slices. The number of point cloud slices at DBH extracted from the Saihanba forest area was the same as the number of measured trees. The point cloud data collected was complete in this forest area led to high extraction accuracy. In the Saihanba forest area, the trees grow regularly and the trunks are straight, which is also an important reason for the high extraction accuracy. The error of the point cloud trunk slice segmentation at the DBH of the two forest areas was caused by the too large parameter setting of the improved K-means algorithm in the process of eliminating branch points and outliers.

The DBH extracted from the Laohugou forest plot and the Saihanba forest plot were close to the measured DBH and highly accurate. The accuracy of the DBH extracted from the Laohugou forest area was lower than that of the Saihanba forest area. This is because there were abnormal values in the DBH extracted from the Laohugou forest plot, and these abnormal parameter values had a greater impact on the accuracy of the overall DBH extraction. There were three main reasons for the error. First, the Laohugou forest area is a natural forest area with a complex terrain environment. When the instrument was set up, the trees blocked each other and some parts of the stems could not be scanned. Due to the large area of the sample plot, there was a phenomenon of blindness when setting up the instrument. A large number of laser spots were returned on the side of the tree close to the scanning position. On the opposite side, it was difficult to receive the returned laser spot. For these trees, the resulting stem points were incomplete and there were missing data, so there was a large error in the extracted DBH (Figure 17). Second, the trunks were irregular and contorted, which affected the accuracy of DBH extraction. Third, due to the tree species, the outer surface of the trunk was irregular, resulting in inconsistencies between the measured DBH and the DBH extracted by point cloud fitting. The method proposed in this paper was used to extract the DBH of white birch and larch. The experimental results show that the accuracy of the DBH extraction of the both trees was very high. For the difference in the accuracy of the DBH of the both trees, we analyzed that it was caused by the lack of data and the tree's own characteristics (trunk and bark). The method of fitting the parameter of DBH through slices can follow four approaches: circle fitting [28], [51], Hough transform [52], [53], cylinder fitting [54]–[56], and ellipse fitting [30], [50], [57]. In this paper, the DBH was extracted using the circle fitting method. We also compared the result with the accuracy of cylindrical fitting, ellipse fitting and Hough transform (Figure 18). The accuracy of cylindrical fitting was close to that of circle fitting when point cloud slices were thick. The error of using ellipse fitting was larger because the shape of these tree diameter slices was quite different from the ellipse. As the thickness of tree diameter slices increases, the number of noise points projected onto the image increases, which reduces the accuracy of Hough transform extraction. The reason why the accuracy of the method in this paper was better than other methods was that we used the improved K-means algorithm to eliminate

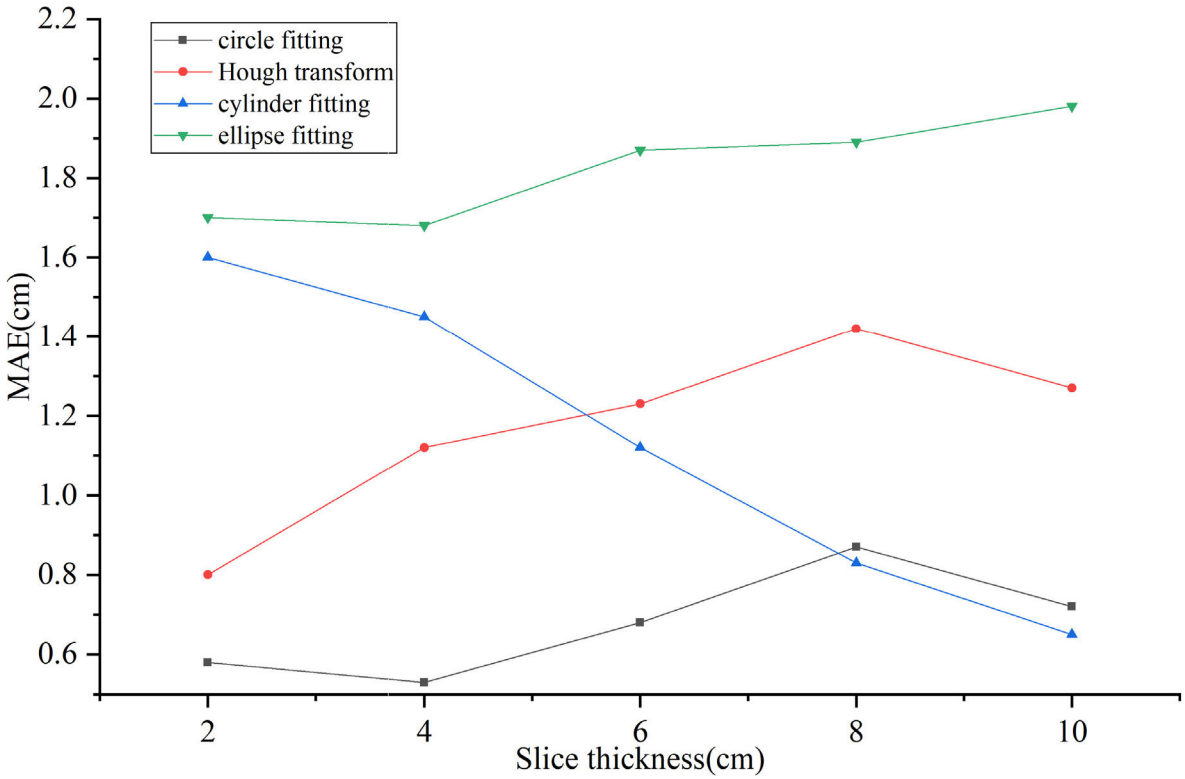

FIGURE 18. Precision comparison of DBH fitting methods.

some error points and outliers. In addition, the selection of DBH fitting method should refer to the shape of tree diameter slices. Fitting the DBH to incompletely sliced point cloud data is a challenge and there is no effective way yet to reduce this error.

V. CONCLUSION

This paper used UAVLS and TLS to collect forest data to extract TH and DBH and presented an automatic extraction algorithm of DBH, which streamlined the extraction process of DBH and increased its accuracy. The point cloud data obtained by UAVLS was performed single tree segmentation to extract the TH, which avoided errors in retrieving the highest tree tops. We sliced the point cloud data obtained by TLS at breast height. The point density analysis algorithm and the least square method were used to automatically extract and fit the DBH of the slice point cloud data. The RMSE of TH extracted from Laohugou forest area and Saihanba forest area were 0.7 m and 0.65 m respectively. The R^2 of two forest areas were greater than 0.94. The MIOU extracted from the slice point cloud of the stem in the two forest areas was 0.89. For the extraction of DBH from Laohugou forest area and Saihanba forest area, the RMSE were 0.65 cm and 0.43 cm respectively and the R^2 were greater than 0.99. The method proposed in this paper also extracts the height and DBH of different tree species in two forest areas. The extraction accuracy of parameters of the two types of trees was very close. Therefore, the method in this paper was also suitable for the extraction of TH and DBH of different tree species. The proposed forest parameters extraction method takes full advantage of different LiDAR instruments to collect data, maximize the accuracy of parameters extraction and provides the impetus for new forestry resource investigation approaches. In the future, we will work on the extraction of parameters for many different types of trees.

REFERENCES

[1] N. Scovronick, M. B. Budolfson, F. Dennig, M. Fleurbaey, A. Siebert, R. H. Socolow, D. Spears, and F. Wagner, "Impact of population growth and population ethics on climate change mitigation policy," *Proc. Nat. Acad. Sci. USA*, vol. 114, no. 46, pp. 12338–12343, Nov. 2017.
[2] L. Al-Ghussain, "Global warming: Review on driving forces and mitigation," *Environ. Prog. Sustain. Energy*, vol. 38, no. 1, pp. 13–21, Jan. 2019.
[3] R. Prăvălie, "Major perturbations in the Earth's forest ecosystems. Possible implications for global warming," *Earth-Sci. Rev.*, vol. 185, pp. 544–571, Oct. 2018.
[4] Y. Wang, M. Lehtomäki, X. Liang, J. Pyörälä, A. Kukko, A. Jaakkola, J. Liu, Z. Feng, R. Chen, and J. Hyyppä, "Is field-measured tree height as reliable as believed—A comparison study of tree height estimates from field measurement, airborne laser scanning and terrestrial laser scanning in a boreal forest," *ISPRS J. Photogramm. Remote Sens.*, vol. 147, pp. 132–145, Jan. 2019.
[5] C. Liu, Y. Xing, J. Duanmu, and X. Tian, "Evaluating different methods for estimating diameter at breast height from terrestrial laser scanning," *Remote Sens.*, vol. 10, no. 4, p. 513, 2018.
[6] P. W. West and P. W. West, *Tree and Forest Measurement*. Cham, Switzerland: Springer, 2009.
[7] X. Liang, J. Hyyppä, H. Kaartinen, M. Lehtomäki, J. Pyörälä, N. Pfeifer, M. Holopainen, G. Brolly, P. Francesco, J. Hackenberg, and H. Huang, "International benchmarking of terrestrial laser scanning approaches for forest inventories," *ISPRS J. Photogram. Remote Sens.*, vol. 144, pp. 137–179, Oct. 2018.

[8] X. Li, J. Xiao, and B. He, "Chlorophyll fluorescence observed by OCO-2 is strongly related to gross primary productivity estimated from flux towers in temperate forests," *Remote Sens. Environ.*, vol. 204, pp. 659–671, Jan. 2018.

[9] T. Sun, J. Qi, and H. Huang, "Discovering forest height changes based on spaceborne lidar data of ICESat-1 in 2005 and ICESat-2 in 2019: A case study in the Beijing-Tianjin-Hebei region of China," *Forest Ecosyst.*, vol. 7, no. 1, pp. 1–12, Dec. 2020.

[10] P. Boucher, S. Hancock, D. Orwig, L. Duncanson, J. Armston, H. Tang, K. Krause, B. Cook, I. Paynter, Z. Li, A. Elmes, and C. Schaaf, "Detecting change in forest structure with simulated GEDI lidar waveforms: A case study of the hemlock woolly adelgid (HWA; *Adelges tsugae*) infestation," *Remote Sens.*, vol. 12, no. 8, p. 1304, Apr. 2020.

[11] L. R. Jarron, N. C. Coops, W. H. MacKenzie, P. Tompalski, and P. Dykstra, "Detection of sub-canopy forest structure using airborne LiDAR," *Remote Sens. Environ.*, vol. 244, Jul. 2020, Art. no. 111770.

[12] Y. Su, Q. Ma, and Q. Guo, "Fine-resolution forest tree height estimation across the Sierra Nevada through the integration of spaceborne LiDAR, airborne LiDAR, and optical imagery," *Int. J. Digit. Earth*, vol. 10, no. 3, pp. 307–323, 2017.

[13] H. Zhou, J. Zhang, L. Ge, X. Yu, Y. Wang, and C. Zhang, "Research on volume prediction of single tree canopy based on three-dimensional (3D) LiDAR and clustering segmentation," *Int. J. Remote Sens.*, vol. 42, no. 2, pp. 738–755, Jan. 2021.

[14] W. Chen, H. Xiang, and K. Moriya, "Individual tree position extraction and structural parameter retrieval based on airborne LiDAR data: Performance evaluation and comparison of four algorithms," *Remote Sens.*, vol. 12, no. 3, p. 571, Feb. 2020.

[15] M. Mielcarek, A. Kamińska, and K. Stereńczak, "Digital aerial photogrammetry (DAP) and airborne laser scanning (ALS) as sources of information about tree height: Comparisons of the accuracy of remote sensing methods for tree height estimation," *Remote Sens.*, vol. 12, no. 11, p. 1808, Jun. 2020.

[16] F. Giannetti, N. Puletti, V. Quatrini, D. Travaglini, F. Bottalico, P. Corona, and G. Chirici, "Integrating terrestrial and airborne laser scanning for the assessment of single-tree attributes in Mediterranean forest stands," *Eur. J. Remote Sens.*, vol. 51, no. 1, pp. 795–807, Jan. 2018.

[17] L. Wallace, R. Musk, and A. Lucieer, "An assessment of the repeatability of automatic forest inventory metrics derived from UAV-borne laser scanning data," *IEEE Trans. Geosci. Remote Sens.*, vol. 52, no. 11, pp. 7160–7169, Nov. 2014.

[18] Q. Xu, B. Li, M. Maltamo, T. Tokola, and Z. Hou, "Predicting tree diameter using allometry described by non-parametric locally-estimated copulas from tree dimensions derived from airborne laser scanning," *Forest Ecol. Manage.*, vol. 434, pp. 205–212, Feb. 2019.

[19] D. Wu, K. Johansen, S. Phinn, and A. Robson, "Suitability of airborne and terrestrial laser scanning for mapping tree crop structural metrics for improved orchard management," *Remote Sens.*, vol. 12, no. 10, p. 1647, May 2020.

[20] A. P. D. Corte, F. E. Rex, D. R. A. D. Almeida, C. R. Sanquetta, C. A. Silva, M. M. Moura, B. Wilkinson, A. M. A. Zambrano, E. M. D. C. Neto, H. F. P. Veras, A. D. Moraes, C. Klauberg, M. Mohan, A. Cardil, and E. N. Broadbent, "Measuring individual tree diameter and height using GatorEye high-density UAV-LiDAR in an integrated crop-livestock-forest system," *Remote Sens.*, vol. 12, no. 5, p. 863, Mar. 2020.

[21] N. A. Husin, S. Khairunniza-Bejo, A. F. Abdullah, M. S. M. Kassim, D. Ahmad, and A. N. N. Azmi, "Application of ground-based LiDAR for analysing oil palm canopy properties on the occurrence of basal stem rot (BSR) disease," *Sci. Rep.*, vol. 10, no. 1, pp. 1–16, Dec. 2020.

[22] I. Indirabai, M. V. H. Nair, J. R. Nair, and R. R. Nidamanuri, "Direct estimation of leaf area index of tropical forests using LiDAR point cloud," *Remote Sens. Applications: Soc. Environ.*, vol. 18, Apr. 2020, Art. no. 100295.

[23] K. Calders, J. Adams, J. Armston, H. Bartholomeus, S. Bauwens, L. P. Bentley, J. Chave, F. M. Danson, M. Demol, M. Disney, R. Gaulton, S. M. Krishna Moorthy, S. R. Levick, N. Saarinen, C. Schaaf, A. Stovall, L. Terryn, P. Wilkes, and H. Verbeeck, "Terrestrial laser scanning in forest ecology: Expanding the horizon," *Remote Sens. Environ.*, vol. 251, Dec. 2020, Art. no. 112102.

[24] T. de Conto, K. Olofsson, E. B. Görgens, L. C. E. Rodriguez, and G. Almeida, "Performance of stem denoising and stem modelling algorithms on single tree point clouds from terrestrial laser scanning," *Comput. Electron. Agricult.*, vol. 143, pp. 165–176, Dec. 2017.

[25] E. Lindberg, J. Holmgren, K. Olofsson, and H. Olsson, "Estimation of stem attributes using a combination of terrestrial and airborne laser scanning," *Eur. J. Forest Res.*, vol. 131, no. 6, pp. 1917–1931, Nov. 2012.

[26] P. Polewski, A. Erickson, W. Yao, N. Coops, P. Krzystek, and U. Stilla, "Object-based coregistration of terrestrial photogrammetric and ALS point clouds in forested areas," *ISPRS Ann. Photogramm., Remote Sens. Spatial Inf. Sci.*, vol. III-3, pp. 347–354, Jun. 2016.

[27] C. Hopkinson, L. Chasmer, C. Young-Pow, and P. Treitz, "Assessing forest metrics with a ground-based scanning LiDAR," *Can. J. Forest Res.*, vol. 34, no. 3, pp. 573–583, 2004.

[28] G. Liu, J. Wang, P. Dong, Y. Chen, and Z. Liu, "Estimating individual tree height and diameter at breast height (DBH) from terrestrial laser scanning (TLS) data at plot level," *Forests*, vol. 9, no. 7, p. 398, Jul. 2018.

[29] M. N. Bazezew, Y. A. Hussin, and E. H. Kloosterman, "Integrating airborne LiDAR and terrestrial laser scanner forest parameters for accurate above-ground biomass/carbon estimation in ayer hitam tropical forest, Malaysia," *Int. J. Appl. Earth Observ. Geoinf.*, vol. 73, pp. 638–652, Dec. 2018.

[30] W. Ye, C. Qian, J. Tang, H. Liu, X. Fan, X. Liang, and H. Zhang, "Improved 3D stem mapping method and elliptic hypothesis-based DBH estimation from terrestrial laser scanning data," *Remote Sens.*, vol. 12, no. 3, p. 352, Jan. 2020.

[31] D. Girardeau-Montaut, "Cloudcompare-open source project," *OpenSource Project*, vol. 588, 2011. [Online]. Available: http://www.cloudcompare.org/

[32] R. B. Rusu and S. Cousins, "3D is here: Point cloud library (PCL)," in *Proc. IEEE Int. Conf. Robot. Autom.*, May 2011, pp. 1–4.

[33] W. Zhang, J. Qi, P. Wan, H. Wang, D. Xie, X. Wang, and G. Yan, "An easy-to-use airborne LiDAR data filtering method based on cloth simulation," *Remote Sens.*, vol. 8, no. 6, p. 501, Jun. 2016.

[34] W. Xiao, A. Zaforemska, M. Smigaj, Y. Wang, and R. Gaulton, "Mean shift segmentation assessment for individual forest tree delineation from airborne LiDAR data," *Remote Sens.*, vol. 11, no. 11, p. 1263, 2019.

[35] E. Ayrey, S. Fraver, J. A. Kershaw, Jr., L. S. Kenefic, D. Hayes, A. R. Weiskittel, and B. E. Roth, "Layer stacking: A novel algorithm for individual forest tree segmentation from LiDAR point clouds," *Can. J. Remote Sens.*, vol. 43, no. 1, pp. 16–27, 2017.

[36] J. Yang, Z. Kang, S. Cheng, Z. Yang, and P. H. Akwensi, "An individual tree segmentation method based on watershed algorithm and three-dimensional spatial distribution analysis from airborne LiDAR point clouds," *IEEE J. Sel. Topics Appl. Earth Observ. Remote Sens.*, vol. 13, pp. 1055–1067, 2020.

[37] A. M. Ramiya, R. R. Nidamanuri, and R. Krishnan, "Individual tree detection from airborne laser scanning data based on supervoxels and local convexity," *Remote Sens. Appl., Soc. Environ.*, vol. 15, Aug. 2019, Art. no. 100242.

[38] N. Chernov and C. Lesort, "Least squares fitting of circles," *J. Math. Imag. Vis.*, vol. 23, no. 3, pp. 239–252, Nov. 2005.

[39] M. K. Jakubowski, Q. Guo, and M. Kelly, "Tradeoffs between LiDAR pulse density and forest measurement accuracy," *Remote Sens. Environ.*, vol. 130, pp. 245–253, Mar. 2013.

[40] V. Thomas, P. Treitz, J. H. McCaughey, and I. Morrison, "Mapping stand-level forest biophysical variables for a mixedwood boreal forest using LiDAR: An examination of scanning density," *Can. J. Res.*, vol. 36, no. 1, pp. 34–47, 2006.

[41] E. Sibona, A. Vitali, F. Meloni, L. Caffo, A. Dotta, E. Lingua, R. Motta, and M. Garbarino, "Direct measurement of tree height provides different results on the assessment of LiDAR accuracy," *Forests*, vol. 8, no. 1, p. 7, Dec. 2016.

[42] K. Stereńczak, M. Mielcarek, B. Wertz, K. Bronisz, G. Zajńczkowski, A. M. Jagodziński, W. Ochał, and M. Skorupski, "Factors influencing the accuracy of ground-based tree-height measurements for major European tree species," *J. Environ. Manage.*, vol. 231, pp. 1284–1292, Feb. 2019.

[43] T. Hilker, M. van Leeuwen, N. C. Coops, M. A. Wulder, G. J. Newnham, D. L. B. Jupp, and D. S. Culvenor, "Comparing canopy metrics derived from terrestrial and airborne laser scanning in a douglas-fir dominated forest stand," *Trees*, vol. 24, no. 5, pp. 819–832, Oct. 2010.

[44] S. Jayathunga, T. Owari, and S. Tsuyuki, "Evaluating the performance of photogrammetric products using fixed-wing UAV imagery over a mixed conifer–broadleaf forest: Comparison with airborne laser scanning," *Remote Sens.*, vol. 10, no. 2, p. 187, Jan. 2018.

[45] M. Mielcarek, K. Stereńczak, and A. Khosravipour, "Testing and evaluating different LiDAR-derived canopy height model generation methods for tree height estimation," *Int. J. Appl. Earth Observ. Geoinf.*, vol. 71, pp. 132–143, Sep. 2018.

[46] L. Cao, H. Liu, X. Fu, Z. Zhang, X. Shen, and H. Ruan, "Comparison of UAV LiDAR and digital aerial photogrammetry point clouds for estimating forest structural attributes in subtropical planted forests," *Forests*, vol. 10, no. 2, p. 145, Feb. 2019.
[47] L. Liu, A. Zhang, S. Xiao, S. Hu, N. He, H. Pang, X. Zhang, and S. Yang, "Single tree segmentation and diameter at breast height estimation with mobile LiDAR," *IEEE Access*, vol. 9, pp. 24314–24325, 2021.
[48] S. M. Beyene, Y. A. Hussin, H. E. Kloosterman, and M. H. Ismail, "Forest inventory and aboveground biomass estimation with terrestrial LiDAR in the tropical forest of Malaysia," *Can. J. Remote Sens.*, vol. 46, no. 2, pp. 130–145, Mar. 2020.
[49] S. Zhou, F. Kang, W. Li, J. Kan, Y. Zheng, and G. He, "Extracting diameter at breast height with a handheld mobile LiDAR system in an outdoor environment," *Sensors*, vol. 19, no. 14, p. 3212, Jul. 2019.
[50] H. Huang, Z. Li, P. Gong, X. Cheng, N. Clinton, C. Cao, W. Ni, and L. Wang, "Automated methods for measuring DBH and tree heights with a commercial scanning lidar," *Photogramm. Eng. Remote Sens.*, vol. 77, no. 3, pp. 219–227, Mar. 2011.
[51] M. Herrero-Huerta, R. Lindenbergh, and P. Rodríguez-Gonzálvez, "Automatic tree parameter extraction by a mobile LiDAR system in an urban context," *PLoS ONE*, vol. 13, no. 4, Apr. 2018, Art. no. e0196004.
[52] T. Aschoff, M. Thies, and H. Spiecker, "Describing forest stands using terrestrial laser-scanning," *Int. Arch. Photogramm., Remote Sens. Spatial Inf. Sci.*, vol. 35, no. 5, pp. 237–241, 2004.
[53] J. Heinzel and M. Huber, "Tree stem diameter estimation from volumetric TLS image data," *Remote Sens.*, vol. 9, no. 6, p. 614, Jun. 2017.
[54] Y. Xie, J. Zhang, X. Chen, S. Pang, H. Zeng, and Z. Shen, "Accuracy assessment and error analysis for diameter at breast height measurement of trees obtained using a novel backpack LiDAR system," *Forest Ecosystems*, vol. 7, no. 1, pp. 1–11, Dec. 2020.
[55] A. S. Antonarakis, "Evaluating forest biometrics obtained from ground LiDAR in complex riparian forests," *Remote Sens. Lett.*, vol. 2, no. 1, pp. 61–70, Mar. 2011.
[56] V. Kankare, X. Liang, M. Vastaranta, X. Yu, M. Holopainen, and J. Hyyppä, "Diameter distribution estimation with laser scanning based multisource single tree inventory," *ISPRS J. Photogramm. Remote Sens.*, vol. 108, pp. 161–171, Oct. 2015.
[57] G. Bu and P. Wang, "Adaptive circle-ellipse fitting method for estimating tree diameter based on single terrestrial laser scanning," *J. Appl. Remote Sens.*, vol. 10, no. 2, Jun. 2016, Art. no. 026040.

JIANCHANG CHEN received the B.S. degree in geographic information science from the Shandong University of Technology, Zibo, Shandong, China, in 2019. He is currently pursuing the M.S. degree in surveying and mapping with Lanzhou Jiaotong University and the Chinese Academy of Surveying and Mapping. His research interests include laser point cloud deep learning and 3-D information extraction.

YIMING CHEN received the Ph.D. degree in cartography and geographical information system from Beijing Normal University, in 2018. He is currently an Assistant Professor Fellow with the Chinese Academy of Surveying and Mapping. His research interest includes air-ground LiDAR data forest resources stereo monitoring survey.

ZHENGJUN LIU received the Ph.D. degree in cartography and geographical information system from the Institute of Remote Sensing and Digital Earth, Chinese Academy of Sciences, in 2003. He is currently a Professor with the Chinese Academy of Surveying and Mapping. His research interests include power line inspection of airborne LiDAR, remote sensing image change detection, and mapping application of LiDAR and multisensory fusion.